IRANIAN JOURNAL OF CATALYSIS

Electrochemical amperometric sensing of loratadine using NiO modified paste electrode as an amplified sensor

Neda Raeisi-Kheirabadi, Alireza Nezamzadeh-Ejhieh*, Hamidreza Aghaei

Department of Chemistry, Shahreza Branch, Islamic Azad University, P.O. Box 311-86145, Shahreza, Isfahan, Iran

ABSTRACT

A modified carbon paste electrode with NiO nanoparticles showed an excellent electrocatalytic behavior towards loratadine in the voltammetric and chronoamperometric approaches. Typical plots of I_C/I_L vs. $t^{1/2}$ were contracted, and an average rate constant of 185.5 ± 2.2 M^{-1} s^{-1} was obtained from the slope of the curve. The geometric surface area of the electrode was 0.0314 cm^2, and an average D-value of $(1.11 \times 10^{-3} \pm 1.16 \times 10^{-4})$ m^2 s^{-1} was obtained for the diffusion of loratadine (Lor) towards the electrode surface. When the effective surface area (0.245 cm^2) was used in calculations, an average D-value of $(1.83 \times 10^{-5} \pm 1.96 \times 10^{-6})$ cm^2 s^{-1} was obtained. ΔI response is the peak current difference of the electrode at a fixed time when Lor analyte was added, and it is in proportion to the loratadine concentration in the range of 20-1000 nM. The limit of detection (LOD) and the limit of quantification (LOQ) of the method were 1.4 and 4.7 nM Lor when the $3S_b/m$ and $10S_b/m$ criteria were used, respectively.

Keywords: Loratadine; Chronoamperometry; Electrocatalysis; Electro-oxidation; Carbon paste electrode

1. Introduction

Catalysis, in general, is a tremendously important field in chemistry that influences the kinetics of the proposed chemical reaction by a change in the mechanism pathway and the decrease in the activation energy of the original catalyst-free reaction [1-12]. So far, to oxidize various organic compounds, some strong inorganic oxidants such as Cr(VI) oxides, permanganate, hypervalent iodine reagents, etc., have been used [13-22]. The application of these oxidizing agents may be limited due to high cost, high toxicity, high corrosiveness, instability, needing a dangerous preparation procedure, and high amounts of residual waste and byproducts. Thus, the application of these oxidants may not be environmentally friendly, and some excess techniques may need to be applied to the recovery and disposal of the resulting waste [23-25]. Further, some halogenated organic solvents and N-chlorosuccinimide organic oxidants suffer from a non-environmentally friendly drawback [26].

Accordingly, great attention has been paid to electrocatalysts. Electrocatalysis is a unique field of electrochemistry that is important in industrial electrochemistry and electrochemical techniques. Electrocatalysis involves an electrochemical reaction by the adsorbed reactant and/or product species [27-30]. Commonly, this electrochemical reaction at the electrode-solution interface can drastically affect the reaction mechanism's kinetics. In this process, the electrochemical reaction proceeds at the electrode surface, which is electrically conductive.

Thus, the kinetics of the process can be controlled by the physicochemical properties of electrochemical interfaces. On the other hand, the nature of the electrode materials and the electrical double layer structure formed at the electrode-solution interface can control the overall kinetics of the electrode process. In electrocatalysis, the crystalline phase of the electrode modifier and the crystallographic orientations of the electrode surface drastically affect the electrode reaction kinetics. For example, for some amino acids, by a change in the electrode materials, the adsorbed configurations and the chiral property can be changed [31,32].

*Corresponding author.
E-mail address: *arnezamzadeh@iaush.ac.ir*
(**A. Nezamzadeh-Ejhieh**)

The catalytic activity of noble metal-based electrocatalysts depends on the metal type and the homogeneity and surface properties. On the other hand, high surface area results in high electrocatalytic activity [33-35]. The Pt and Pt-based alloys have been widely used in the electrocatalysis field, but their applications may be limited due to high cost and poisoning effects. For example, poisoning of Pt-based catalysts by CO species in the fuel cells occupies the active centers on the electrode surface and decreases the catalytic activity. Accordingly, the poisoning effect is well known as a significant drawback of the noble metal-based electrocatalysts for the electro-reduction or electro-oxidation of various chemicals [36-46].

Thus, introduced novel electrocatalysts such as metal oxides [47-49], silver halides [50], etc., have been used as effective electrocatalysts. A metal oxide with high electrocatalytic activity is a p-type NiO semiconductor with a bandgap energy of about 3.6-4.0 eV. It has impressive electrical conductivity, high electrochromic efficiency, high electro-activity, high effective surface area, cheap and straightforward synthesis procedures, and a wide modulation range. Due to these great futures, NiO acts as a good electron mediator in many electrochemical sensors. It has been widely used in photocatalysis, supercapacitors, lithium-ion batteries, dye sensitizer in solar cells, transparent electrodes, biosensors, etc. [51-53]. The unusual electrocatalytic activity of NiO has been related to the Ni(II)/Ni(III) redox couple in the modified electrodes by NiO [54-59]. Accordingly, we used a modified carbon paste electrode (CPE) with NiO, and its electrocatalytic activity was evaluated towards the voltammetric determination of sulfasalazine [60]. The effects of the calcination temperature in the preparation of NiO nanoparticles (NPs) were studied on the electrocatalytic activity of the modified NiO-CPE electrode. The results showed that the modified electrode with NiO NPs calcined at 200 °C had the best photocatalytic activity.

Further, the electrocatalytic activity of the modified NiO-CPE was tested towards loratadine (Lor) in a cyclic voltammetry approach, and the kinetic aspects of the process were evaluated [61]. Here, to complete the work, the electrocatalytic behavior of the modified NiO-CPE electrode will illustrate towards Lor in a chronoamperometric approach.

Histamine is the primary source of allergic disorders such as asthma, urticarial, and allergic rhinitis, and these are the most common human diseases [62,63]. Loratadine is a tricyclic antihistamine that has been widely used for treating seasonal allergic symptoms. It potentially locks the effects of the naturally formed histamine. It mitigates the symptoms of allergies such as hay fever and urticarial, including skin rash, itching, sneezing, hives, watery eyes, and runny nose, etc. [62-64]. Loratadine has some side effects such as headache, feeling tired or sleepy, dizziness, nervousness (in children), and GI distress (diarrhea, abdominal pain, nausea, and vomiting). These anticholinergic effects may cause sedation (rare side effects), mydriasis, and xerostomia for loratadine [65,66]. Based on this illustration, the monitoring and control of loratadine are essential to achieve successful treatment, increase the safety of the patients using this drug, and reduce its side effects. Thus, the modified NiO-CPE electrode was used for the chronoamperometric determination of Lor in work.

2. Experimental

2.1. Chemicals and solutions

Loratadine (Lor) (99.9%), $Ni(CH_3COO)_2.4H_2O$ (99.9%), citric acid (99.9%), graphite powder (99.99%), Nujol oil (99.99%), and other required chemicals with analytical purity were obtained from the Flucka/Aldrich company. Triply distilled deionized water was used for preparing the solutions. In the voltammetric and chronoamperometric experiments, a 0.1 M NaOH supporting electrolyte was used.

A 0.5 µM Lor stocks solution was prepared daily and used to prepare the diluter solution using the serial dilution approach [61]. A pharmaceutical tablet of loratadine (10 mg) was purchased from Poorsina Pharmacy Company (Tehran, Iran) to prepare a real sample solution. One pulverized tablet was accurately weighed (100 mg) and completely powdered by hand-mixing in an agate mortar. Then, an aliquot of the powder (19.1 mg) was poured into a 50 mL volumetric flask and dissolved in 5 mL ethanol after 5 min sonication. The resulting solution reached the mark of 0.1 M NaOH solution [62].

For NiO synthesis, 2.5 g nickel (II) acetate was added in a 100 mL beaker and completely dissolved in 50 mL water. Then, 1.92 g citric acid (CA) was added to another beaker. After the dropwise addition of solution A to CA solution, the solution pH was adjusted to 3-3.5 by HNO_3 to achieve a clear solution. The solution temperature was adjusted to 65 °C and stirred to reach a highly viscous residual. It was then air-dried to produce a light green gel precursor. Finally, the gel was calcined at 200 °C for 6 h to achieve NiO NPs [60,61,67,68].

For preparing the raw and modified carbon paste (CP), Nujol oil was added to the aliquot amount of graphite powder to obtain a 10 w% Nujol oil. For example, for 1 g carbon powder, 0.1 g of oil should be added. After hand-mixing in an agate mortar for 15 min, the paste

was the raw CP [69]. For modifying the paste by NiO NPs, a definite weight of NiO NPs was added to a definite amount of the raw CP to achieve 5-20 w% of NiO modifier in the paste. The mixtures were then hand-mixed thoroughly in an agate mortar for another 15 min to achieve a homogeneous modified NiO-CP matrix [61].

The modified carbon paste electrode (NiO NPs-CPE) was prepared in the following procedure, which is illustrated in the literature [61,69,70]. An aliquot of the modified NiO-CP was added to the end of an insulin syringe and fully compressed by mechanical force. A copper wire was pushed into the end of the syringe to achieve electrical contact. The modified NiO-CPE electrodes with different amounts of NiO-modifier have then been used in the cyclic voltammetry and chronoamperometry techniques. The raw CPE electrode was also prepared in the same method by using the raw CP. When the electrode response tended to diminish, the electrode surface was polished with a soft paper to achieve a renewed surface [61,69,70].

2.2. Apparatus and CV/CA procedures

A Field Emission Scanning Electron Microscope (FESEM; Mira 3-XMU) was used to sample characterization. pH adjustments were done by a Jenway p-ion meter (model 3505) [61].

The cyclic voltammetric (CV) and chronoamperometric (CA) experiments were carried out by a potentiostat/galvanostat (Autolab, PGSTAT-101, EcoChemie, Netherlands), with data acquisition NOVA 1.8 software. Here, a three-electrode voltammetric cell system was used, which contained an Ag/AgCl reference electrode (Azar Electrode Com, Iran), the modified NiO-CPE working electrode, and a platinum counter (auxiliary) electrode. Before each CV or CA run, the test solution was purged by high pure nitrogen gas for 5 min [61].

All CV and CA runs were carried out in triplicate measurements. The CV and CA of the Lor test solutions were recorded by the raw CPE and the modified NiO-CPE electrodes. The electrode response was the Δi value, which is the difference between the raw and the modified electrodes [61].

3. Result and Discussion

3.1. A summary of the characterization results

NiO NPs, raw and modified CPEs were identified by some characterization techniques, for which results have been illustrated in the first section of the work [61]. Here, brief results obtained in the characterization techniques are reported as follow. A hexagonal crystalline structure was observed for the carbon paste

(JCPDS: 00-026-1076), while NiO calcined at 200 °C showed an amorphous phase. Applying the Scherrer equation on the XRD data showed an average crystallite size of 36 nm for the NiO-CP sample. In comparison, about 42 nm was obtained as an average crystallite size when the Williamson-Hall equation was applied to the XRD data [61].

Some SEM pictures of the raw CPE and the modified NiO-CPE electrodes are shown in Fig. 1. Fig. 1 A and B show a plate-like morphology for the prepared carbon paste in the raw CPE, which remained unchanged after modifying the paste with NiO NPs (images C and D). These images have good agreement with the images reported in the first section of the work [61]. As shown in the images of the modified electrode, the plate-like CP was covered by semi-spherical NiO NPs. EDX analysis of the NiO-CPE showed the 10 w% Ni in the modified paste. The homogeneity of the modified paste was confirmed by the X-ray mapping images, as illustrated in the first part of the work [61].

3.2. Catalytic behavior of the modified electrode

Typical cyclic voltammograms (CVs) of the raw CPE and the proposed NiO-CPE modified electrode were recorded in the potential range of -0.5 to 0.7 V (vs. Ag/AgCl), and the results are depicted in Fig. 2A-B. As shown, both acidic (0.1 M HCl) and neutral (0.1 M KCl) supporting electrolytes showed no significant peak current for the modified electrode in the absence and presence of Lor analyte (Fig. 2A). At the same time, strong alkaline pHs (0.1 M NaOH) caused a significant voltammetric current. Based on the results, increased pHs towards the strong alkaline values caused an increased voltammetric current for the modified electrode. The NiO modifier can be oxidized to Ni(III) as O=Ni-OH• species in the strong alkaline pHs at the anodic peak potential of about 480 mV. In the reverse scan, the Ni(III)/Ni(II) reduction process mainly occurs at about 345 mV. This electrode process needs high amounts of hydroxyl anions in the media. Thus, the neutral and acidic pHs are not suitable. In strong acidic pHs (0.1 M), partial dissolution of NiO at the electrode surface may occur. In KCl supporting electrolyte, chloride anions may attach to the NiO species and partially bonds the Ni(III) in the electrooxidized O=Ni-OH• species. This relatively facilitates the electro-oxidation of NiO to O=Ni-OH•, and thus, a partial voltammetric current has flowed for the modified electrode.

A comparison of CVs in Fig. 2A,B shows a drastically enhanced peak current in 0.1 M NaOH supporting electrolyte, which was enhanced by adding loratadine into the solution.
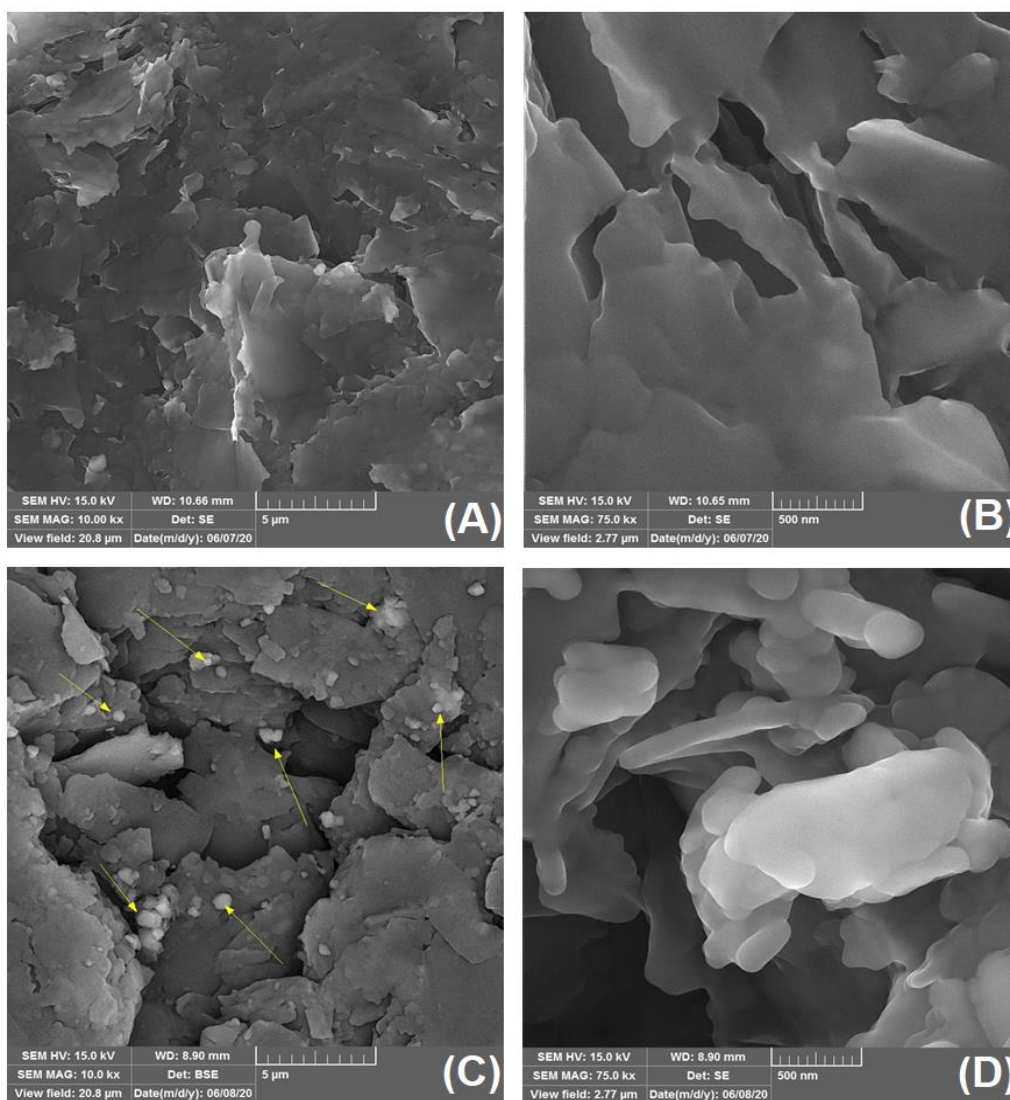
Fig. 1. SEM images for the raw CPE (A,B) and the modified NiO-CPE (C,D) electrodes [61].

This catalytic current is due to the reaction of loratadine with the electrogenerated O=Ni-OH• species, which regenerates NiO species as the initial reactant for the forward electrode process [61, 71,72]. One mechanism for the oxidation of loratadine is the oxidation of the nitrogen atom of the pyridine ring by the electrogenerated O=Ni-OH• species [61].

3.3. Effective surface area for the CPE electrode

Each electrode has two surface areas, including the geometric and effective area. As we know, the porosity of the electrode surface plays a drastic role in the electrochemical response of the electrode. In contrast, the effective surface area of the electrode drastically depends on the porosity of the surface. Thus, the electrochemical response of each electrochemical sensor depends on the effective surface area of the electrode. The raw CPE electrode had an internal diameter of 1 mm, resulting in a geometric surface area

of 0.0314 cm^2. To estimate the effective surface area, typical CVs for the CPE in 0.5 mM K$_3$Fe(CN)$_6$ solution containing 0.5 M KCl supporting electrolyte were recorded at different scan rates from 5 to 30 mV/s. The results are shown in Fig. 3. Based on the CV results, the I$_{(p)c}$ and I$_{p(a)}$ versus the $\nu^{1/2}$ were constructed, and the results are shown in Fig. 3B. The linear relationship of the plots confirms a diffusion-controlled process for the electrode response by using the following reaction [73,74].

$$\text{Fe(CN)}_6{}^{3-} \rightleftharpoons \text{Fe(CN)}_6{}^{2-} + \text{e} \qquad \textbf{(1)}$$

For calculating the effective surface area, we used the following equation in which A is the effective surface area (A$_{eff}$), C is the concentration of the proposed electroactive species in media (here 0.5 mM K$_3$Fe(CN)$_6$), υ is the scan rate, and D is the diffusion coefficient of the electroactive species participated in the electrode response [75].
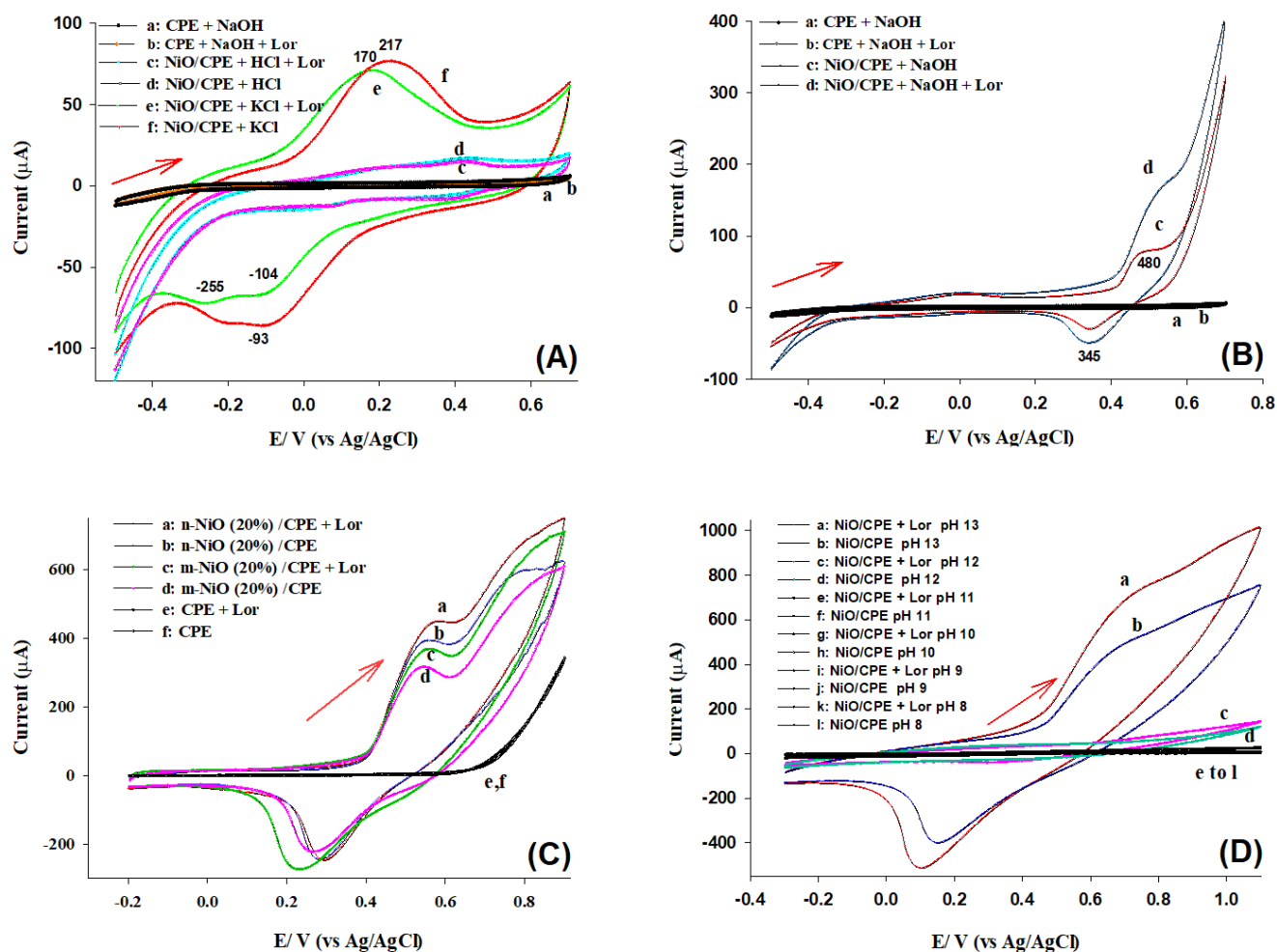
Fig. 2. (A,B) CVs of the NiO-CPE in different supporting electrolytes towards loratadine: Conditions: 0.5 μM Lor, υ = 50 mV/s, 20% modifier, and 0.1 M supporting electrolytes; **(C)** The effects of the nano and bulk NiO modifier on the CV response of the modified NiO-CPE electrode; **(D)** The effects of the pH of NaOH solution on the CV response of the modified electrode response in conditions mentioned in the case (A) [61].
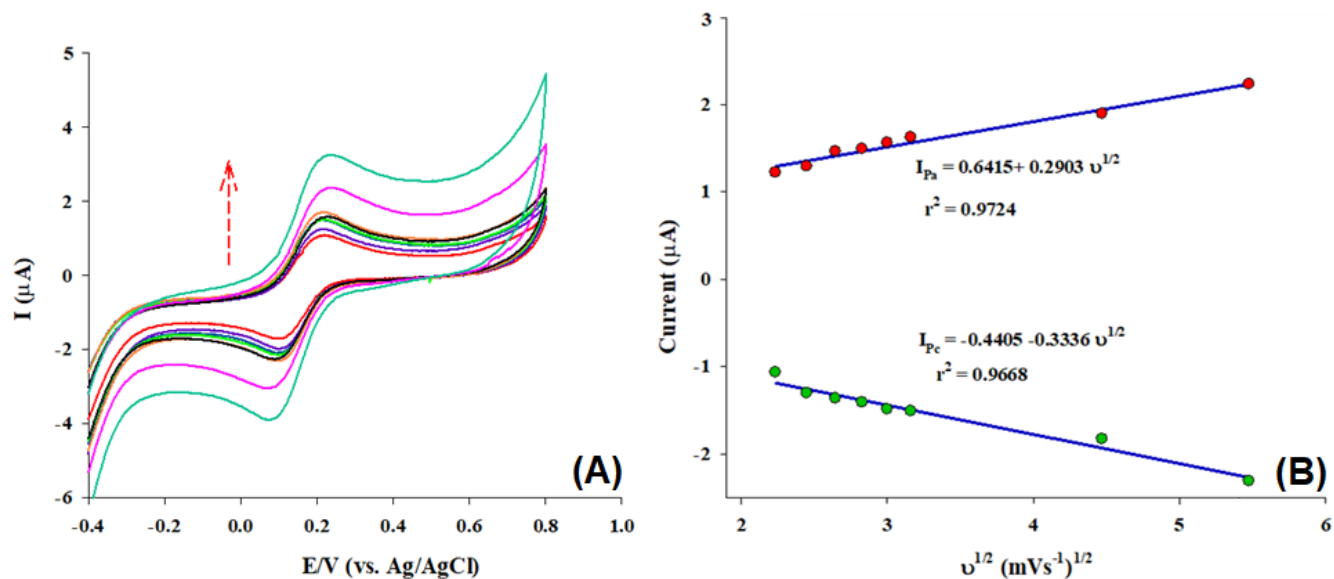

Fig. 3. (A) CVs obtained for the raw CPE in various scan rates (5 to 30 mV/s) in 0.5 mM $K_3Fe(CN)_6$ + 0.5 M KCl supporting electrolyte; **(B)** The linear behavior for the plot of peak current versus scan rate square root.

In the applied conditions, the relative D-value of 8.3×10^{-5} cm^2 s^{-1} for the $Fe(CN)_6^{3-}$ electroactive species has been reported in the literature [76].

$$I_P = 2.69 \times 10^5 \, n^{3/2} \, A \, D^{1/2} \, C \, \upsilon^{1/2} \qquad (2)$$

The slopes of the curves in Fig. 3B were used for calculating the A_{eff} for the raw CPE electrode. By using the slope of the anodic curve, an effective surface area of 0.245 cm^2 was estimated for the used CPE electrode, which is much higher than the geometric value (0.0314 cm^2).

3.4. Chronoamperometric results

chronoamperometry is a proper electrochemical technique. The working electrode's potential is fixed at a value that is suitable for initiating the faradaic processes at the electrode surface (caused by the potential step) to monitor the resulting current during the time. Both single and double potential step approaches can be applied to the working electrode to carry out the chronoamperometric measurements. Some information can be obtained about the identity of the electrolyzed species by the ratio of the anodic peak current to the cathodic peak current. Like all pulsed techniques, chronoamperometry has high charging currents exponential decay against time as any RC circuit. In this technique, the decay trend for the Faradaic current obeys the Cottrell equation. Commonly, the charging current decay is much faster than the decay for the Faradic current. Due to the integration of the current over relatively long-time intervals, a better S/N ratio can be achieved by chronoamperometry when comprised of other aerometric techniques [75,77].

Like more electrochemical cells, a three-electrode system is used for chronoamperometric measurements. Two common types of chronoamperometry are controlled-potential chronoamperometry and controlled-current chronoamperometry. A CV run can be run before running controlled-potential chronoamperometry to determine the peak potential for the analytes. In general, a fixed area of the electrode will be used in chronoamperometry, which is suitable for evaluating the electrode processes of the coupled chemical reactions. This is especially useful for studying the reaction mechanism in organic electrochemistry [75, 78, 79].

Chronoamperometric runs were performed using the modified NiO-CPE electrode in the absence and presence of Lor at a fixed potential value of 0.6 V obtained from CVs in a three-electrode system. The obtained chronoamperograms are shown in Fig. 4A. As the results show, no response was achieved by applying the raw CPE in 0.1 M NaOH supporting electrolyte. Further, the CPE showed no considerable response in the presence of Lor. When the modified electrode was immersed in the working solution (containing Lor analyte), the electrochemical current was increased, which agrees with the catalytic current confirmed by CVs in the sections above-mentioned. As shown, by an increase in the concentration of loratadine, the catalytic current was increased.

Some chronoamperograms were selected for the study of the kinetics of the electrode process by using the following Galuse equation in which I_C and I_L are the catalytic and limiting currents of loratadine at the NiO-CPE/CPE, respectively, k is the rate constant for the electrode process, and C is the concentration of Lor [80-82]. The I_C is the current difference in the absence and presence of Lor. Typical plots of I_C/I_L vs. $t^{1/2}$ were constructed, as shown in Fig. 4B. From the slopes of the curves, an average rate constant of 185.5 ± 2.2 M^{-1} s^{-1} was calculated for the electrocatalytic reaction of Lor at the surface of the modified NiO-CPE electrode.

$$I_C/I_L = [\pi \, (k.C.t)]^{1/2} \qquad (3)$$

The Cottrell equation is defined by the following formula, in which 'n' is the number of electrons involved in the Faradic reaction, A is the electrode surface area, and D is the diffusion coefficient of the analyte towards the diffusion layer at the electrode surface [75]. Based on the Cottrell equation and the corresponding chronoamperogram, typical I versus $t^{1/2}$ were constructed and shown in Fig. 4C. An average D-value of $(1.11 \times 10^{-3} \pm 1.16 \times 10^{-4})$ m^2 s^{-1} was obtained from the slopes of the curves and the geometric surface area of the electrode (0.0314 cm^2), for the diffusion of Lor towards the electrode surface. An average D-value of $(1.83 \times 10^{-5} \pm 1.96 \times 10^{-6})$ cm^2 s^{-1} was obtained, when the effective surface area (0.245 cm^2) was used in calculations. The latter value is more reliable and real because the effective surface area is responsible for the electrode process and the created chronoamperometric or voltammetric current. Higher D-value based on the geometric area has a mathematical reason because we used the same (which was created by the effective surface area) slope in both calculations. But when we used a smaller D-value in the denominator of the used equation ($D^{1/2} = (Slope)/(n.F.A.C.\pi^{-1/2}.t^{-1/2})$), a higher D-value would be expected.

$$I = n.F.A.D^{1/2}.C.\pi^{-1/2}.t^{-1/2} \qquad (4)$$

A loratadine D-value of 6.64×10^{-4} cm^2 s^{-1} has been reported in a 0.50 M HClO$_4$ solution by chronoamperometry using a boron-doped diamond electrode with a geometric area of 0.30 cm^2 [83].
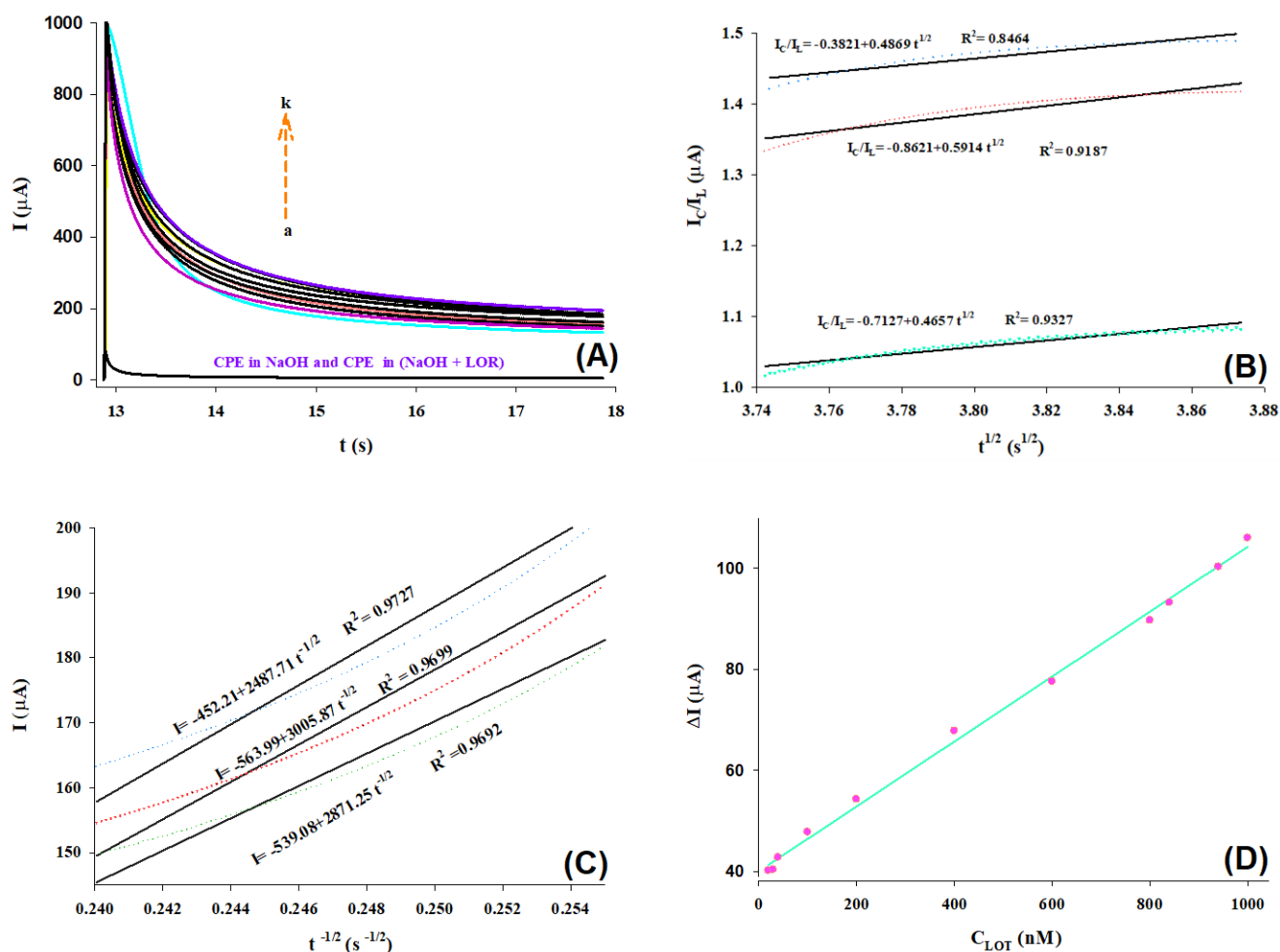
Fig. 4. (A) Chronoamperograms of NiO/CPE in 0.1 M NaOH solution containing different concentrations of LOT (from down to up corresponds to 20 – 1000 nM); **(B)** variation of I_C/I_L versus $t^{1/2}$ obtained from chronoamperograms; **(C)** variation of current versus $t^{-1/2}$ obtained from chronoamperograms A); **(D)** Typical calibration curve obtained for the quantitative determination of LOT in chronoamperometric approach.

Due to the proportional dependence of the chronoamperometric current on the Lor concentration, this method was used to quantitate loratadine. A typical calibration curve is shown in Fig. 4D, which shows the linear plot of $\Delta I = 0.064C + 40.086$ (R^2=0.9969). ΔI is the current difference of the electrode at a t=13.09 s by adding Lor. As shown, a proportional relationship between the ΔI and Lor concentration is obtained in the range of 20-1000 nM. The limit of detection (LOD) and the limit of quantification (LOQ) of the method were 1.4 and 4.7 nM Lor when the $3S_b/m$ and $10S_b/m$ criteria were used, respectively. S_b is the average of blank response (1 mL H_2O + 24 mL NaOH (0.1 M)) based on 10 replicate measurements about $2.19 \times 10^{-4} \pm 2.84 \times 10^{-5}$ nA. The results confirm that the proposed modified NiO-CPE electrode is beneficial for the quantitative determination of trace amounts of loratadine by chronoamperometry.

4. Conclusions

The CV peak current of the modified NiO-CPE electrode was increased by adding loratadine to the test solution. This confirms an electrocatalytic behavior for the modified electrode towards loratadine. This increased current drastically depends on the solution pH because the oxidation of NiO to NiOOH takes place in high alkaline pH about 12-13. Based on this electrocatalytic behavior, the modified electrode was used in the chronoamperometric study of the work, and an average rate constant of 185.5 ± 2.2 M^{-1} s^{-1} was obtained. Based on the geometric surface area (0.0314 cm^2), an average D-value of ($1.11 \times 10^{-3} \pm 1.16 \times 10^{-4}$) m^2 s^{-1} was obtained for the diffusion of loratadine towards the electrode surface. This value was smaller than the D-value of $1.83 \times 10^{-5} \pm 1.96 \times 10^{-6}$ cm^2 s^{-1} calculated by the effective surface area (0.245 cm^2).

References

[1] N. Pourshirband, A. Nezamzadeh-Ejhieh, S. N. Mirsattari, Chem. Phys. Lett. 761 (2020) 138090.

[2] A. R. Massah, R. J. Kalbasi, S. Kaviyani, RSC Adv. 3 (2013) 12816-12825.

[3] M. Mehrali-Afjani, A. Nezamzadeh-Ejhieh, H. Aghaei, Chem. Phys. Lett. 759 (2020) 137873.

[4] M. Ghiaci, R.N. Esfahani, H. Aghaei, Catal. Commun. 10 (2009) 777-780.

[5] L. Khazdooz, A. Zarei, T. Ahmadi, H. Aghaei, L. Golestanifar, N. Sheikhan, Res. Chem. Intermed. 44 (2018) 93-115.

[6] H. Aghaei, M. Ghiaci, Reac. Kinet. Mech. Cat. 131 (2020) 233–246.

[7] M. Masteri-Farahani, P. Eghbali, E. Şahin, Colloids Surf. A 570 (2019) 347-353.

[8] H. Aghaei, A. Yasinian, A. Taghizadeh, 178 (2021) 569-579.

[9] P. Eghbali, M.U. Gürbüz, A.S. Ertürk, Ö. Metin. Inter. J. Hydrogen Energy 45 (2020) 26274-26285.

[10] H. Aghaei, M. Ghavi, G. Hashemkhani, M. Keshavarz, Int. J. Biol. Macromol. 162 (2020) 74-83.

[11] R. Pankaj, A. A. Parwaz Khan, P. Singh, Sep. Purif. Technol. 247 (2020) 116957.

[12] M. Ghiaci, R.J. Kalbasi, H. Aghaei, Catal. Commun. 8 (2007) 1843-1850.

[13] V. Mathan Raj, L. R. Ganapathy Subramanian, S. Thiyagarajan, V. Edwin Geo, Fuel 234 (2018) 934-943.

[14] I. Rossetti, C. Biffia, L. Bianchi, V. Nichele, M. Signoretto, F. Menegazzo, E. Finocchio, G. Ramis, A. Di Michele, Appl. Catal. B 117–118 (2012) 384–396

[15] W. Yang, X. Zhang, J. Su, Y. Wang, Q. Zhao, J. Zhou, Fuel Proc. Technol. 179 (2018) 108-113.

[16] C. H. Bartholomew, Appl. Catal. A 212 (2001) 17–60

[17] S. Sheik Mansoor, S. Syed Shafi, J. Mol. Liq. 155 (2010) 85-90.

[18] Piet W.N.M. van Leeuwen, Appl. Catal. A 212 (2001) 61–81.

[19] F. Javadi, R. Tayebee, Iran J. Catal. 7 (2017) 283-292.

[20] F. Shirini; M. Abedini; M. Shamsi-Sani; M. Seddighi, Iran. J. Catal. 5 (2017) 223-230.

[21] A. Bamoniri, A. Pourali, Seyed M. R. Nazifi, Iran. J. Catal. 4 (2014) 261-265.

[22] J. Safaei-Ghomi, H. Shahbazi-Alavi, M. R. Saberi-Moghadam, A. Ziarati, Iran. J. Catal. 4 (2014) 289-294.

[23] I. Mohammad, S. Mohsin, S. Muhammad, Chin. Sci. Bull 58 (2013) 2354-2359.

[24] I. Ibrahim Kan, A. Mehmet Kutc, Turk. J. Chem. 36 (2012) 827-840.

[25] H. Karimi-Maleh, A. Ayati, S. Ghanbari, Y. Orooji, B. Tanhaei, F. Karimi, M. Alizadeh, J. Rouhi, L. Fu, M. Sillanpää, J. Mol. Liq. 329 (2021) 115062.

[26] T. Tamiji, A. Nezamzadeh-Ejhieh, J. Taiwan Inst. Chem. Eng. 104 (2019) 130-138.

[27] H. Karimi-Maleh, M. Lütfi Yola, N. Atar, Y. Orooji, F. Karimi, P. Senthil Kumar, J. Rouhi, M. Baghayeri, J. Colloid Interface Sci. 592 (2021) 174–185.

[28] F. Tahernejad-Javazmi, M. Shabani-Nooshabadi, H. Karimi-Maleh, Talanta 176 (2018) 208-213.

[29] H. Karimi-Maleh, K. Cellat, K. Arıkan, A. Savk, F. Karimi, F. Şen, Mater. Chem. Phys. 250 (2020) 123042.

[30] H. Karimi- Maleh, F. Karimi, M. Alizadeh, A. L. Sanati, Chem. Rec. 20 (2020) 682-692.

[31] C. F. Zinola, M. E. Martins, E. P. Tejera, N. P. Neves, 2012 (2012) 874687.

[32] Y. Holade, K. Servat, S. Tingry, T. W. Napporn, H. Remita, D. Cornu, K. B. Kokoh, ChemPhysChem 18 (2017) 2573-2605.

[33] H. Karimi-Maleh, M. Alizadeh, Y. Orooji, F. Karimi, M. Baghayeri, J. Rouhi, S. Tajik, H. Beitollahi, S. Agarwal, V.K. Gupta, S. Rajendran, S. Rostamnia, L. Fu, F. Saberi-Movahed, S. Malekmohammadi, Ind. Eng. Chem. Res. 60 (2021) 816-823.

[34] S. A. R. Alavi-Tabari, M. A. Khalilzadeh, H. Karimi-Maleh, J. Electroanal. Chem. 811 (2018) 84-88.

[35] H. Karimi-Maleh, M. Sheikhshoaie, I. Sheikhshoaie, M. Ranjbar, J. Alizadeh, N. Wendy Maxakato, A. Abbaspourrad, New J. Chem. 43 (2019) 2362-2367.

[36] Sh. Sun, L. Sun, Sh. Xi, Y. Du, M.U. Anu Prathap, Z. Wang, Q. Zhang, A. Fisher, Zh. J. Xu, Electrochim. Acta 228 (2017) 183-194.

[37] M. H. Nobahari, A. N. Golikand, M. Bagherzadeh, Iran. J. Catal. 7 (2017) 327-335.

[38] Y. Zhang, F. Gao, P. Song, J. Wang, J. Guo, Y. Shiraishi, Y. Du, ACS Sustainable Chem. Eng. 7 (2019) 3176-3184.

[39] P. Song, H. Xu, J. Wang, Y. Zhang, G. Fei, R. Fangfang, S. Yukihide, W. Caiqin, Y. Du, J. Taiwan Inst. Chem. Eng. 93 (2018) 616-624.

[40] F. Gao, Y. Zhang, P. Song, J. Wang, C. Wang, J. Guo, Y. Du, J. Power Sources 418 (2019) 186–192.

[41] H. Ashassi-Sorkhabi, B. Rezaei-Moghadam, E. Asghari, R. Bagheri, R. Kabiri, J. Taiwan Inst. Chem. Eng. 69 (2016) 118-130.

[42] E. Tavakolian, J. Tashkhourian, Z. Razmi, H. Kazemi, M. Hosseini-Sarvari, Sensors Actuators B 230 (2016) 87-93.

[43] F. Gao, Y. Zhang, P. Song, J. Wang, T. Song, C. Wang, L. Song, Y. Shiraishi, Y. Du, J. Mater. Chem. A 7 (2019) 7891-7896.

[44] A. Ehsani, M. Hadi, E. Kowsari, S. Doostikhah, J. Torabian, Iran. J. Catal. 7 (2017) 187-192.

[45] M. Zhiani, S. Majidi, H. Rostami, M. Mohammadi Taghiabadi, Int. J. Hydrogen Energy, 40 (2015) 568-576.

[46] H. Meixner, U. Lampe, Sensors Actuators B 33 (1996) 198-202.

[47] P. Falcaro, R. Ricco, A. Yazdi, I. Imaz, S. Furukawa, D. Maspoch, R. Ameloot, J.D. Evans, C. J. Doonan, Chem. Rev. 307(2016) 237-254.

[48] I. E. Wachs, Catal. Today 27 (1996) 437-455.

[49] M. E. Franke, T. J. Koplin, U. Simon, Nano. Micro Small 2 (2006) 36-50.

[50] T. Tamiji, A. Nezamzadeh-Ejhieh, Mater. Chem. Phys. 237 (2019) 121813.

[51] M. Miraki, H. Karimi-Maleh, M. A. Taher, S. Cheraghi, F. Karimi, Shilpi Agarwal, V. K. Gupta, J. Mol. Liq. 278 (2019) 672-676.

[52] Y. Akbarian, M. Shabani-Nooshabadi, H. Karimi-Maleh, Sensors Actuators B 273 (2018) 228-233.

[53] F. Iazdani, A. Nezamzadeh-Ejhieh, Spectrochim. Acta Part A 250 (2021) 119228

[54] M. Fouladgar, H. Karimi-Maleh, V. Kumar Gupta, J. Mol. Liq. 208 (2015) 78-83.

[55] Q. Zhou, A. Umar, E. M. Sodki, A. Amine, L. Xu, Y. Gui, A. A. Ibrahim, R. Kumar, S. Baskoutas, Sensors Actuators. B 256 (2018) 604-615.

[56] M. S. Alnarabiji, O. Tantawi, A. Ramli, N. A. Mohd Zabidi, O. B. Ghanem, B. Abdullah, Renew. Sustainable Energy Rev. 114 (2019) 109326.

[57] R. Ahmed, Ghulam Nabi, J. Energy Storage 33 (2021) 102115.

[58] J. Safari, S. Gandomi-Ravandi, J. Iran. Chem. Soc. 12 (2015) 147–154.

[59] H. A. Ariyanta, T. A. Ivandini, Y. Yulizar, J. Mol. Struct. 1227 (2021) 129543.

[60] Z. Amani-Beni, A. Nezamzadeh-Ejhieh, Anal. Chim. Acta 1031 (2018) 47-59.

[61] N. Raeisi-Kheirabadi, A. Nezamzadeh-Ejhieh, H. Aghaei, Microchem. J. 162 (2021) 105869.

[62] M. G. Buckley, C. Walters, W. M. Wong, M. I. D. Cawley, S. Ren, L. B. Schwartz, A. F. Walls, Mast Cell Clin. Sci. 93 (1997) 363–370.

[63] F. Simons, K. Simons, New Engl. J. Med. 330 (1994) 1663-1670.

[64] M. Peyrovi, M.R. Hadjmohammadi, J. Chromatogr. B 980 (2014) 41–47.

[65] I. Cardelús, F. Antón, J. Beleta, J. M. Palacios. Eur. J. Pharmacol. 374 (1999) 249-254.

[66] R. F. Orzechowski, D. S. Currie, C. A. Valancius. Eur. J. Pharmacol. 506 (2005) 257-264.

[67] J. Huang, N. Zhu, T. Yang, T. Zhang, P. Wu, Z. Dang, Biosens. Bioelectron. 7 (2015) 332-339.

[68] F. Fazlali, A. Mahjoub, R. Abazari, Solid State Sci. 48 (2015) 263-269.

[69] N. Pourshirband, A. Nezamzadeh-Ejhieh, Solid State Sci. 99 (2020) 106082.

[70] M. Nosuhi, A. Nezamzadeh-Ejhieh, Electrochim. Acta 223 (2017) 47–62.

[71] M. Shahid, C. He, S. Basu, Inter. J. Hydrogen Energy 19 (2020) 11287-11296.

[72] C. Xu, Z. Tian, P. Shen, S. P. Jiang, Electrochim. Acta 53 (2008) 2610–2618.

[73] S. Sharifian, A. Nezamzadeh-Ejhieh, Mater. Sci. Eng. C 58 (2016) 510–520.

[74] X.-Z. Chen, M. J. Coady, F. Jackson, A. Berteloot, J. Y. Lapointe, Biophys. J. (1995) 2405-2414.

[75] A. J. Bard, L. R. Faulkner, Electrochemical Methods: Fundamentals and Applications, Second Edition, Wiley, 2000.

[76] R. Karimi Shervedani, M. Bagherzadeh, Sensors Actuators B 139 (2009) 657-664.

[77] P. Kissinger, W. R. Heineman, Laboratory Techniques in Electroanalytical Chemistry, Second Edition, CRC Press, 1996.

[78] C. G. Zoski, Handbook of Electrochemistry, Elsevier Science, 2007.

[79] J. M. Seveant, E. Vianello, Electrochim. Acta 10 (1965) 905–920.

[80] Z. Galus, Fundamentals of Electrochemical Analysis, Ellis Horwood, New York, 1976.

[81] M. S. Tohidi, A. Nezamzadeh-Ejhieh, Int. J. Hydrogen Energy 41 (2016) 8881-8892.

[82] A. Nezamzadeh-Ejhieh, H. Hashemi, Talanta 88 (2012) 201-208.

[83] A. P. Pires Eisele, E. Romão Sartori, Anal. Methods 7 (2015) 8697-8703.